

# Al–Zn base alloys with dual-phase microstructure

U. HEROLD-SCHMIDT

*Institut für Werkstoffe, Ruhr-Universität Bochum, Bochum, West Germany*

Al–55 wt % Zn alloys with copper or magnesium additions were subjected to various thermo-mechanical treatments and analysed by microscopy, hardness measurements, and tensile tests. A set of different microstructures was produced exhibiting characteristic features of a dual-phase structure: about 30 vol % of a harder zinc-rich phase are dispersed in a softer aluminium-rich matrix. Small amounts of additional compounds such as  $\tau$ -(Al, Zn, Cu),  $\epsilon$ -CuZn<sub>4</sub>, or  $\alpha''$ -(Al, Zn) could be obtained by various precipitation reactions. It is shown that the combination of conventional precipitation hardening with the new type of microstructure offers promising possibilities for the development of aluminium-base alloys with high deformability and strength.

## 1. Introduction

A dual-phase microstructure (DPM) is characterized by a coarse dispersion of about 30 vol % of a harder component in a softer matrix [1]. In steels this special type of a coarse ferrite-martensite microstructure leads to a favourable combination of high plastic deformability and high ultimate tensile strength. It results from a relatively low yield point followed by a high rate of work hardening. Plastic deformation takes place almost exclusively in the soft ferrite phase while the harder martensite phase provides favourable effects on its work hardening behaviour [2]. This type of microstructure meets well the requirements for the production of high-strength sheet materials.

Among the few aluminium-alloy systems suitable for the production of a DPM with comparable mechanical properties, Al–Zn alloys have recently been found to be most promising [3]. In almost all aluminium-base alloys only two-phase equilibria exist between aluminium solid solutions and brittle intermetallic compounds [4]. Contrary to this, the Al–Zn system is characterized by a two-phase field where two solid solutions (fcc aluminium-rich  $\alpha$  and hcp zinc-rich  $\beta$ ) coexist in a wide range of chemical composition (Fig. 1a). In addition, a metastable miscibility gap ( $\alpha' + \alpha''$ ) is located in the ( $\alpha + \beta$ )-region [5]. It represents

the continuation of the stable gap ( $\alpha_1 + \alpha_2$ ) existing above the eutectoid temperature. Research in the Al–Zn system was mainly concerned with the formation of metastable coherent particles  $\alpha''$  and their transition to the stable  $\beta$ -phase [6]. Another focal point of research was directed towards ( $\alpha + \beta$ )-micro-duplex structures which have to be distinguished from a dual-phase structure. They contain equal volume fractions of both phases with equal grain size and random arrangement to each other. Such microstructures are obtained at eutectoid composition (about 78 wt % Zn) and exhibit superplastic flow at elevated temperatures [7].

For the first time, a DPM containing a dispersion of about 30 vol %  $\beta$  in an  $\alpha$ -matrix was produced by Hornbogen and Turwitt [3]. An Al–55 wt % Zn alloy was subjected to various thermo-mechanical treatments. After homogenization at 400°C no supersaturated  $\alpha$ -solid solution is obtained. Continuous decomposition into ( $\alpha' + \alpha''$ ) as well as discontinuous precipitation of  $\beta$  start immediately at ambient temperature. During annealing at  $T \geq 200^\circ\text{C}$ , the hard and brittle metastable ( $\alpha' + \alpha''$ )-mixture is dissolved by completion of the discontinuous reaction. Simultaneously, discontinuous coarsening of the lamellar microstructure starts. High amounts of cold work followed by further annealing at 200°C result in

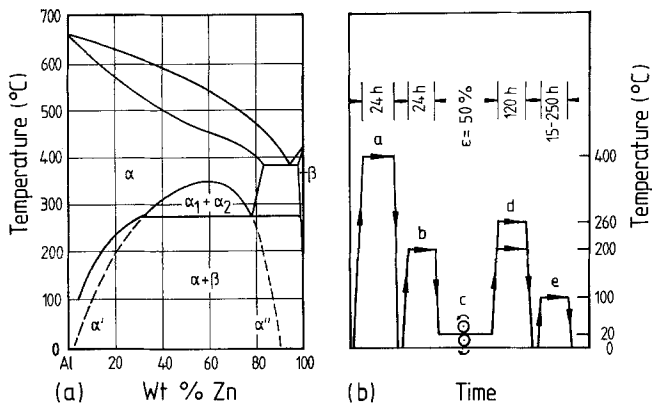


Figure 1 (a) Al-Zn phase diagram, (b) schematic representation of thermomechanical treatments: a, homogenization; b, pretreatment for cold work; c, rolling; d, dual-phase annealing; e, ageing.

a uniform dispersion of equiaxed  $\beta$  grains in  $\alpha$ , due to a combined coagulation and recrystallization reaction. The mechanical properties of this microstructure are characterized by low yield stress ( $Rp_{0.2} = 150$  MPa) and high uniform elongation ( $Ag = 55\%$ ) with a tendency towards superplasticity at ambient temperature. However, the work hardening behaviour and ultimate tensile strength ( $Rm = 185$  MPa) are insufficient as compared to dual-phase steels. Observations of the deformation behaviour indicate that the small work hardening rate is caused by large amounts of grain-boundary sliding and dynamic recovery in the interior of  $\alpha$  and  $\beta$  grains.

It is the aim of the present work to improve the mechanical properties of an Al-55 wt% Zn alloy with DPM by small additions of copper or magnesium. About 1 wt% copper or magnesium can be dissolved in the Al(Zn)-solid solution during homogenization of the master alloy [8, 9]. By suitable thermo-mechanical treatments various metastable and stable intermetallic compounds are expected to precipitate during the production of the DPM. Principally, this should lead to:

1. increased strength of the zinc-rich phase  $\beta$ ;
2. improved work hardening ability of the aluminium-rich phase  $\alpha$ ;
3. stabilization of grain and phase boundaries, i.e. stability against recrystallization, grain growth, grain-boundary sliding.

## 2. Experimental procedure

The alloys used in the present work are summarized in Table I (nominal compositions). Copper-containing specimens are mixtures of pure elements (purity  $> 99.9\%$ ), whereas magnesium-alloyed samples were obtained by diluting an Al-54 wt% Zn-2 wt% Mg-master alloy with aluminium and zinc. Ingots of about 2 kg, were produced by induction melting in an argon atmosphere.

The thermo-mechanical treatments necessary for the particular microstructures are represented schematically in Fig. 1b. After each annealing step the specimens were quenched in water and stored below room temperature.

Conventional light- (LM), scanning electron- (SEM), and transmission electron microscopy (TEM) were applied for the microstructural investigations. TEM-samples were prepared using standard electropolishing techniques supplemented by ion-milling. X-ray diffraction and microdiffraction in TEM were used for phase identification.

Tensile tests were performed with flat specimens of 1.5 mm thickness and 28 mm gauge length at room temperature. The strain rate was fixed at  $3.3 \times 10^{-4} \text{ sec}^{-1}$ . For micro- and macrohardness measurements loads of  $5 \times 10^{-2}$  and 50 N, respectively, were applied.

TABLE I Nominal compositions of alloys studied

	Alloy designation					
	A	B	C	D	E	F
Additions to 55 Zn, balance Al (wt %)	0.1 Cu	0.5 Cu	1 Cu	0.05 Mg	0.1 Mg	1 Mg

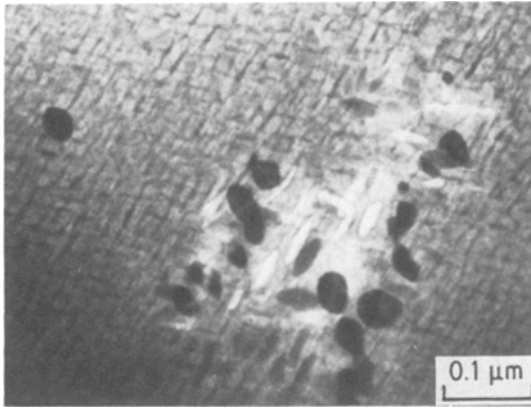


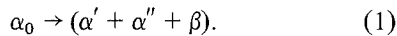
Figure 2 Alloy C, 24 h 400° C: precipitation of coherent  $\alpha''$  and incoherent  $\beta$  (TEM).

### 3. Results

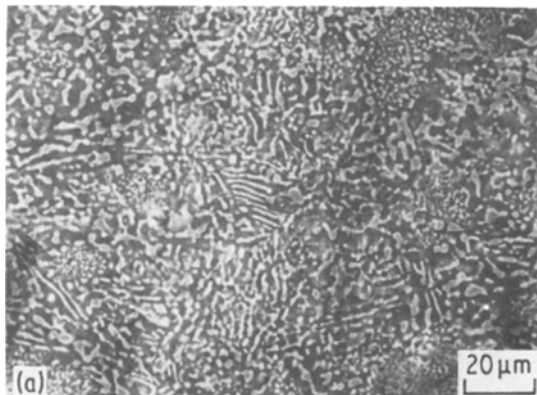
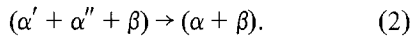
#### 3.1. Copper-containing alloys

The microstructures obtained after various thermo-mechanical treatments (cf. Fig. 1b) are shown in Figs. 2 to 5.

As reported for Al–55 wt % Zn [3] immediately after quenching from the homogenization temperature, a metastable coherent mixture of aluminium-rich  $\alpha'$  and zinc-rich  $\alpha''$  is observed. The  $\{111\}$ -habit of the  $\alpha''$ -plates is well known for Al–Zn alloys [6]. Locally zinc-rich  $\beta$ -particles have formed (Fig. 2):



The first annealing at 200° C (pretreatment for cold work) leads to the discontinuous precipitation of  $\beta$  starting at grain boundaries. In the grains a dispersion of  $\beta$  resulting from continuous precipitation is found (Figs. 3a and b):

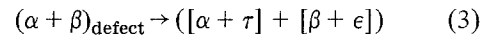


A dual-phase microstructure is obtained after cold work ( $\sim 50\%$  thickness reduction by rolling) followed by a second annealing at 200° C. As in the binary alloy [3] about 30 vol % globular  $\beta$  are dispersed in an  $\alpha$  subgrain structure (Fig. 4a). Most of the  $\beta$ -particles are located at junctions of subgrain boundaries (Fig. 4b). Two additional compounds arise during the combined coagulation and recrystallization reaction:

1. the ternary  $\tau$ -(Al, Zn, Cu)-compound [8] precipitates along the sub-boundaries of  $\alpha$  by heterogeneous nucleation at boundary dislocations (Figs. 4c and d). The volume fraction of  $\tau$  increases with increasing copper-content;

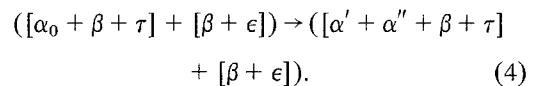
2. the  $\beta$ -grains exhibit a mottled appearance (Fig. 4b). By micro-diffraction, reflections different from those of Zn are revealed. Although no thorough elaboration was made it is assumed that small  $\epsilon$ -CuZn<sub>4</sub>-precipitates have formed in  $\beta$ .

The reactions mentioned above can be summarized as follows:



No further microstructural changes are observed after subsequent ageing at 100° C.

By raising the temperature of the second annealing from 200° C to 260° C (cf. Fig. 1b) only a minor change of the DPM is observed. In addition to the  $\tau$ -phase, small zinc-particles precipitate at the  $\alpha$ -sub-boundaries. Subsequent ageing at 100° C leads to coherent precipitation of spherical G.P. zones in the  $\alpha$ -subgrains (Fig. 5a). After further ageing, plate-shaped  $\alpha''$ -particles appear (Fig. 5b):



The plate thickness increases up to  $\sim 30$  nm

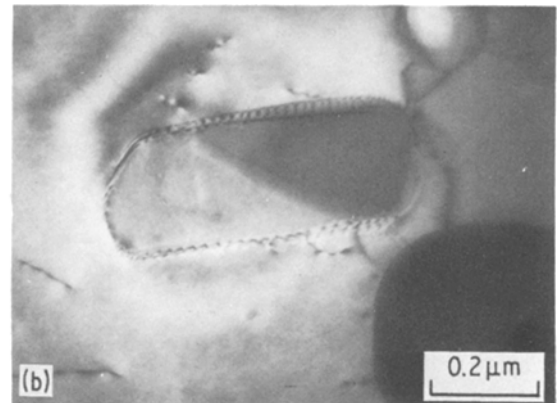
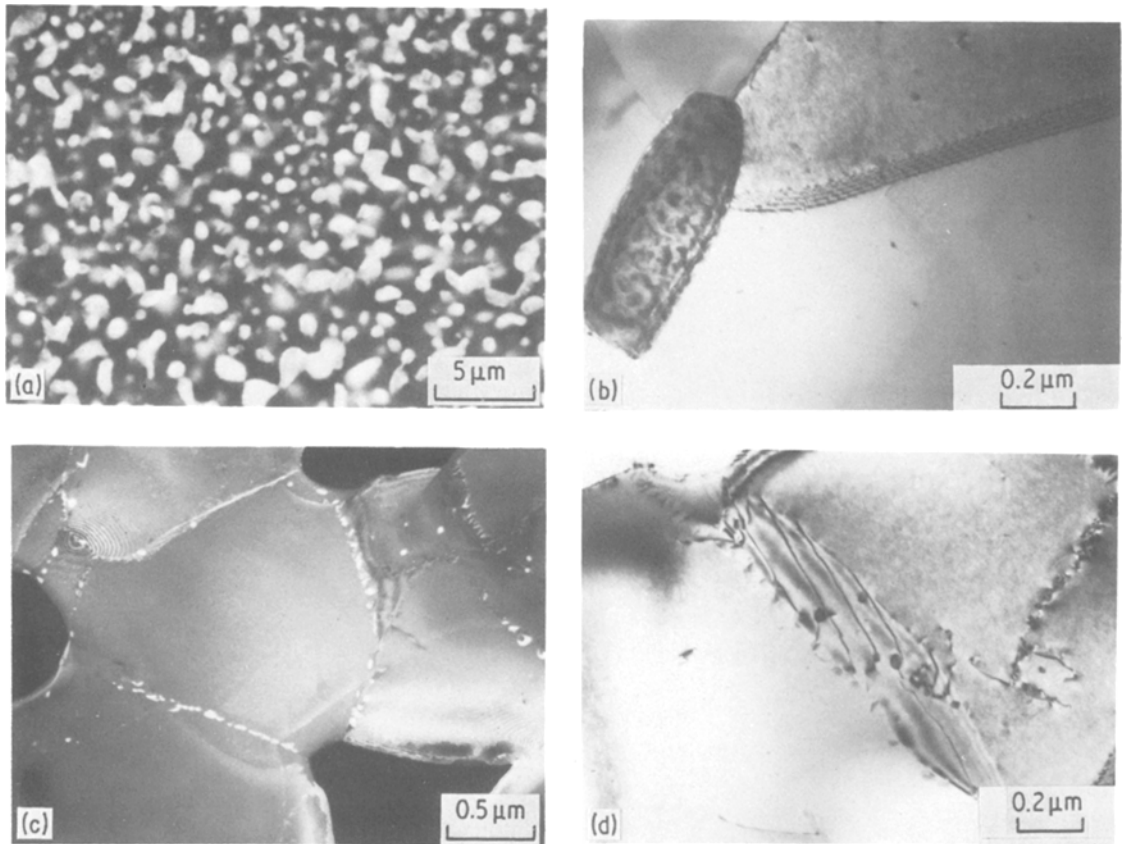
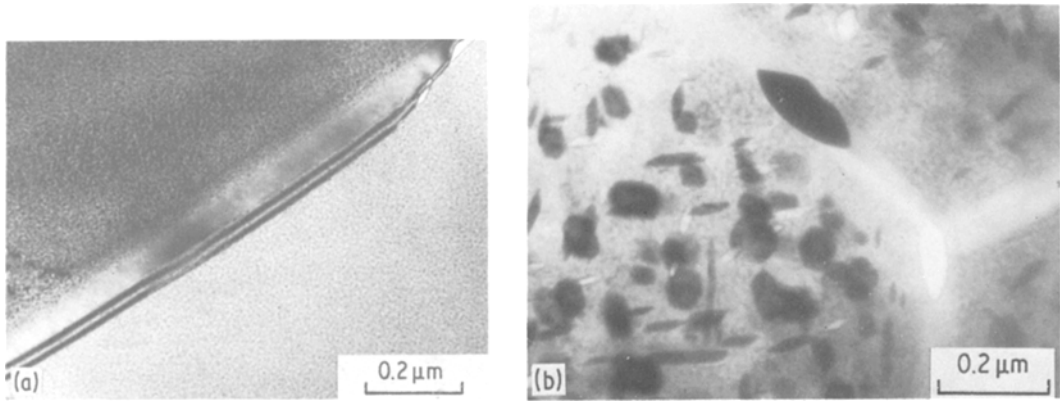


Figure 3 Alloy C, 24 h 400° C + 24 h 200° C: discontinuous and continuous precipitation of  $\beta$ : (a) SEM; (b) TEM.



*Figure 4* Alloy C, 24 h 400° C + 24 h 200° C +  $\epsilon = 50\%$  + 120 h 200° C: (a) dual-phase microstructure (SEM after deep etching; bright: zinc-rich phase, dark: aluminium-rich phase); (b) precipitation of  $\beta$  (dark grain) at sub-boundary junctions of  $\alpha$  (TEM); (c) precipitation of  $\tau$  at sub-boundaries (TEM dark-field with  $\tau$ -reflection); (d)  $\tau$  at boundary dislocations (TEM).



*Figure 5* Alloy C, 24 h 400° C + 24 h 200° C +  $\epsilon = 50\%$  + 120 h 260° C. (a) + 15 h 100° C: formation of spherical  $\alpha''$ -G.P. zones (TEM). (b) + 80 h 100° C: mixture of spherical and plate-shaped  $\alpha''$ ; the large particle at the boundary is  $\beta$  (TEM).

TABLE II Designation of DPM (X represents the DPM in the binary Al–55 wt % Zn alloy [3])

	Microstructure designation				
	1	2	3	4	X
Pretreatment	24 h 400° C 24 h 200° C $\epsilon = 50\%$	24 h 400° C 24 h 200° C $\epsilon = 50\%$	24 h 400° C 24 h 200° C $\epsilon = 50\%$	24 h 400° C 24 h 200° C $\epsilon = 50\%$	24 h 400° C 1 h 200° C $\epsilon = 90\%$
Final treatment	120 h 200° C	120 h 200° C 15–250 h 100° C	120 h 260° C	120 h 260° C 15–250 h 100° C	120 h 200° C
Phases in DPM	$[\alpha + \tau]$ $+ [\beta + \epsilon]$	$[\alpha + \tau]$ $+ [\beta + \epsilon]$	$[\alpha_0 + \beta + \tau]$ $+ [\beta + \epsilon]$	$[\alpha' + \alpha'' + \beta + \tau]$ $+ [\beta + \epsilon]$	$[\alpha] + [\beta]$

after 250 h at 100° C. Precipitate-free zones are found along the subboundaries. Their width ranges from ~100 nm (16 h, 100° C) to ~300 nm (250 h, 100° C). Table II summarizes the treatments used to obtain the different DPM described above.

The macrohardness of the different DPM depends on the alloy composition and heat treatment and varies between 60 and 130 HV<sub>5</sub> (Fig. 6). The corresponding hardness of the binary Al–Zn–DPM amounts to 55 HV<sub>5</sub> [3]. Owing to the very small average grain size ( $d < 5 \mu\text{m}$ ) it was impossible to measure the individual hardness of the aluminium- and zinc-rich phases by microhardness testing.

Tensile tests were conducted only for a few selected DPM. The nominal stress–strain plots are presented in Fig. 7. In comparison with the binary Al–Zn alloy, significant improvements of the yield stress as well as of the work hardening rate are observed. The most promising result is

obtained for a DPM containing 1 wt % copper produced at 260° C and aged to peak hardness (80 h, 100° C).

### 3.2. Magnesium-containing alloys

As in the copper-containing alloys, no homogeneous Al(Zn, Mg)-solid solution is obtained after homogenization. In addition to  $\alpha'$ ,  $\alpha''$ , and  $\beta$ , a fine grained ( $\alpha + \eta\text{-MgZn}_2$ )-mixture appears at the grain boundaries which presumably has already formed during solidification (Fig. 8). Even more MgZn<sub>2</sub> appears after the first annealing at 200° C. The precipitation of small  $\eta$ -crystals takes place in  $\alpha$  during the discontinuous precipitation of  $\beta$  (Fig. 9). Probably the heterogeneous nucleation of  $\eta$  is favoured by the reaction front.

It is impossible to obtain a DPM from this kind of microstructure. Even at the lowest magnesium content, cold rolling without crack formation is limited to about 25% thickness reduction. As reported for the binary Al–Zn alloy [3], the

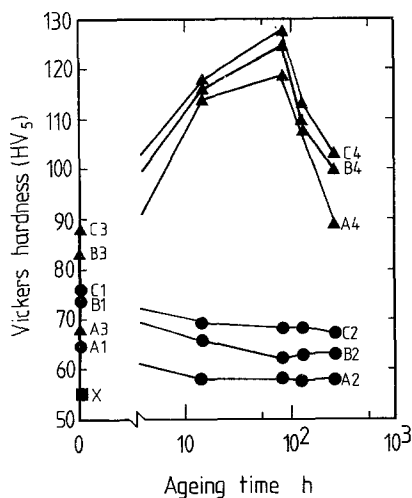


Figure 6 Hardness of various DPM in unaged and aged condition (cf. Table II).

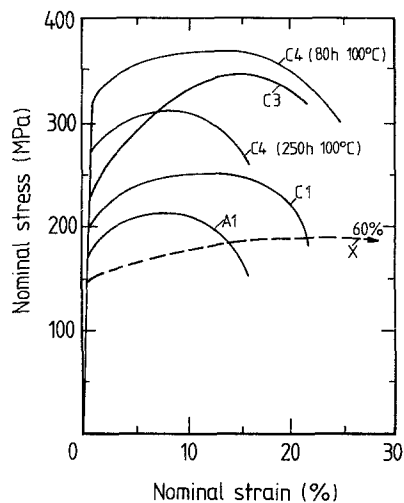


Figure 7 Stress–strain plots of selected DPM (cf. Table II).

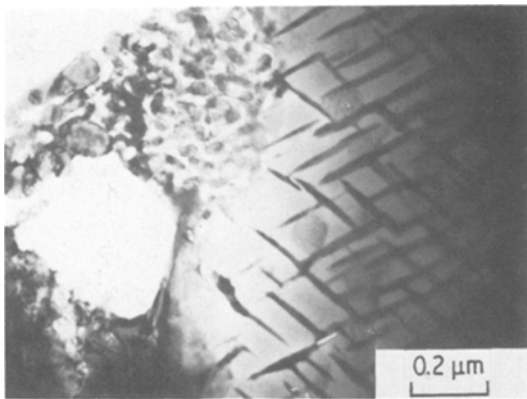


Figure 8 Alloy F, 24 h 400° C: precipitation of  $\alpha''$ ; along grain boundaries (left) a mixture of  $(\alpha + \eta)$  (TEM).

recrystallization reaction induced by this low degree of deformation is insufficient to change the lamellar microstructure into a globular one during the second 200° C annealing.

#### 4. Discussion

A set of different microstructures (1 to 4) has been produced in Al–Zn–Cu alloys by various thermo-mechanical treatments. All exhibit characteristic features of a DPM, i.e. they contain about 30 vol% zinc-rich grains dispersed in a softer aluminium-rich matrix. The most complex microstructure (4) is shown schematically in Fig. 10.

In comparison with the DPM produced in binary Al–Zn [3], a significant difference was noted: precipitation hardening is possible as in many commercial aluminium-base alloys. This results (a) from the addition of copper, and (b)

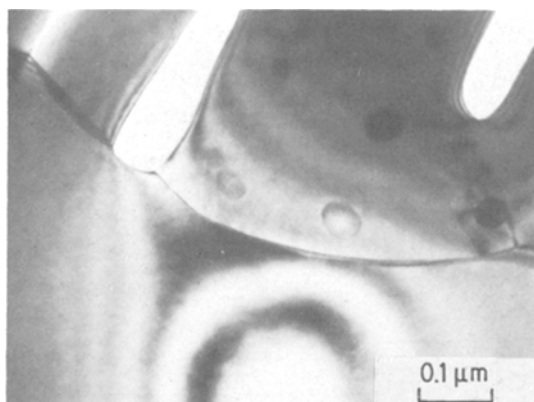


Figure 9 Alloy D, 24 h 400° C + 24 h 200° C: discontinuous precipitation of  $\beta$  and continuous precipitation of small  $\eta$ -crystals (TEM; due to preferred etching of zinc-rich phases holes represent the original  $\beta$ -sites).

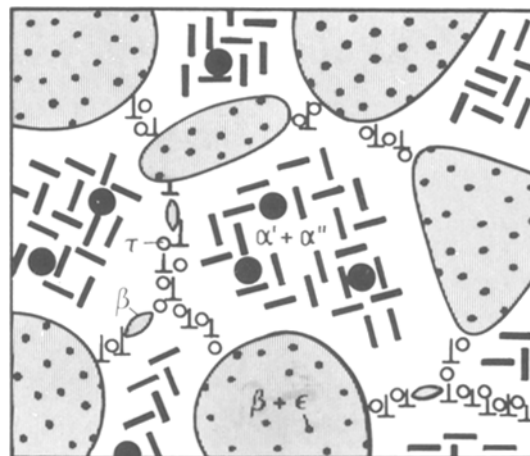


Figure 10 Schematic representation of microstructural elements in a typical dual-phase structure (DPM 4).

from a different thermomechanical treatment. As a consequence, in addition to the aluminium- and zinc-rich solid solutions,  $\alpha$  and  $\beta$ , three more compounds are obtained:  $\tau$ -(Al, Zn, Cu),  $\epsilon$ -CuZn<sub>4</sub>,  $\alpha''$ -(Al, Zn) (cf. Table II).

According to the equilibrium diagram [8] the formation of the Cu–Al-rich  $\tau$ -phase is expected at 200° C as well as at 260° C. However, there is evidence for nucleation difficulties inhibiting its precipitation during the first 200° C annealing. Fig. 4d shows that the dislocation network created during cold work and the second 200° C (260° C) heat treatment serves as a nucleation site for the  $\tau$ -phase. The favourable effect of this nucleation behaviour will be mentioned below.

The precipitation of  $\epsilon$ -CuZn<sub>4</sub> from supersaturated Zn(Cu)-solid solutions is well known for commercial zinc-alloys [10]. Compared to pure zinc, even small amounts of  $\epsilon$  are reported to increase the hardness and tensile strength by about 100%.

In the DPM produced at 260° C age-hardening by  $\alpha''$ -(Al, Zn) precipitation is possible. This can be attributed to the supersaturation of the aluminium-solid solution with zinc. According to the stable Al–Zn-phase diagram (Fig. 1a) about 26 wt % Zn are frozen-in after quenching from 260° C. This concentration is located well inside the metastable miscibility gap during ageing at 100° C [5]. The observed precipitation sequence corresponds to that reported for Al–Zn alloys with comparable zinc contents [5, 11]. The early decomposition stages (Fig. 5a) resemble those observed by Laslaz and Guyot [12] which are presumably governed by a spinodal mechanism. The precipitate free

zones at the sub-boundaries may arise from the depletion of zinc due to the  $\tau$ - and  $\beta$ -precipitation as well as from a reduced vacancy concentration.

Hardness measurements reflect the precipitation sequence (Fig. 6): The underaged condition is characterized by coherent spherical G.P. zones (Fig. 5a); the peak hardness corresponds to a mixture of spherical and plate-shaped zones (Fig. 5b), and in the overaged condition larger plates (thickness  $> 10$  nm) appear. They are generally considered as incoherent [13].

Contrary to this, TEM observations as well as hardness measurements indicate that during ageing of DPM produced at  $200^\circ\text{C}$  no G.P. zone formation occurs. The aluminium solid solution should contain at least 13 wt% Zn which still leads to decomposition in alloys with comparable compositions [14]. However, the vacancy concentration is presumably very small as the DPM are quenched from temperatures as low as  $200^\circ\text{C}$ . Thus it is supposed that the combination of low vacancy and zinc-concentrations is responsible for the observed microstructural stability.

The precipitation reactions mentioned above strongly influence the mechanical properties of the DPM (Fig. 7). Compared to the binary Al–Zn alloy [3] the formation of  $\epsilon$  and  $\tau$  in the microstructures Al to Cl raises the yield stress and improves the work hardening ability. The former effect can be attributed mainly to the precipitation hardening of the zinc-rich phase by  $\epsilon$  and increases with copper content. Work hardening is caused by pinning of  $\alpha$ -sub-boundaries by  $\tau$  during plastic deformation. However, a significant reduction of the uniform elongation cannot be avoided. The additional precipitation of zinc at sub-boundaries in DPM produced at  $260^\circ\text{C}$  but not aged (A3 to C3) further increases the work-hardening rate. The mixture of coherent and incoherent  $\alpha''$  in peak aged specimens (A4 to C4/80 h,  $100^\circ\text{C}$ ) leads to the highest yield stress and ultimate tensile strength accompanied by the best uniform elongation. The overaged condition (A4 to C4/250 h,  $100^\circ\text{C}$ ) was expected to exhibit an even better work-hardening ability due to the higher amount of incoherent  $\alpha''$ . However, the results suggest that the wide precipitation-free zones observed in those specimens lead to localized softening and failure.

## 5. Conclusions

1. The combination of a new type of microstructure, the dual-phase structure, with conventional precipitation hardening offers promising

possibilities for the development of aluminium-base alloys with high deformability and strength.

2. Al–55 wt% Zn alloys with copper additions have proved to be suitable for the production of the required complex microstructures. The mechanical properties achieved are still comparable with commercial aluminium base alloys. However, there is a tendency for high uniform elongation which can only be obtained by this special type of microstructure.

3. It is impossible to produce DPM in the magnesium-containing alloys. Even very low additions lead to a severe embrittlement by  $\text{MgZn}_2$  even during the thermo-mechanical pretreatments which would be required to obtain the desired microstructure.

## Acknowledgements

The author wishes to thank Professor E. Hornbogen for helpful suggestions and critical reading of the manuscript. The preparation of the master alloys by the Vereinigte Aluminiumwerke, Bonn, FRG as well as financial support by the Stifterverband Metalle, FRG are gratefully acknowledged.

## References

1. J. BECKER, E. HORNBOGEN and P. STRATMANN, *Z. Metallkde.* **71** (1980) 27.
2. J. BECKER, X. CHENG and E. HORNBOGEN, *Z. Werkstofftechn.* **12** (1981) 301.
3. E. HORNBOGEN and M. TURWITT, *Metall.* **37** (1983) 1208.
4. J. C. JACQUET and H. WARLIMONT, *Z. Metallkde.* **72** (1981) 13, 82, 169.
5. V. GEROLD and W. SCHWEIZER, *ibid.* **52** (1961) 76.
6. A. KELLY and R. B. NICHOLSON, "Progress in Materials Science", Vol. 10, edited by B. Chalmers (Pergamon Press, Oxford, 1966) p. 149.
7. K. A. PADMANABHAN and G. J. DAVIS, "Superplasticity" (Springer, Berlin, 1980).
8. L. A. WILLEY, "Metals Handbook", Vol. 8, edited by T. Lyman (ASM, Metals Park, Ohio, 1973) p. 386.
9. W. KÖSTER and W. DULLENKOPF, *Z. Metallkde.* **28** (1936) 363.
10. DEUTSCHE ZINKBERATUNG (ED.), "Zink-Taschenbuch", (Metall-Verlag, Berlin, 1981) p. 76.
11. A. ZAHRA, C. Y. ZAHRA and J. MATHIEU, *Z. Metallkde.* **71** (1980) 54.
12. G. LASLAZ and P. GUYOT, *Acta Metall.* **25** (1977) 277.
13. R. GRAF and B. GENTY, *Compt. Rend.* **251** (1960) 2517.
14. A. JUNQUA, J. MIMAULT and J. DELAFOND, *Acta Metall.* **24** (1976) 779.

Received 8 May  
and accepted 1 June 1984